jet INTL JOURNAL OF ELECTRONICS AND TELECOMMUNICATIONS, 2024, VOL. 70, NO. 4, PP. 997–1003
Manuscript received June 12, 2024; revised October 2024. doi: 10.24425/ijet.2024.152087

The development of algorithms for safe control of an autonomous ship

Monika Rybczak, and Agnieszka Lazarowska

***Abstract*—The paper presents the results of a research on the development of algorithms for ship's safe ship trajectory calculation and automatic control of the ship along the determined trajectory. These methods are intended for use in the autonomous navigation system of an Unmanned Surface Vehicle (USV) or a Maritime Autonomous Surface Ship (MASS). The work presents the consecutive stages of a research that must be carried out in order to develop a system that will perform the task of multidimensional ship control in a port. The safe trajectory is calculated with the use of the Ant Colony Optimization (ACO) method. The ship motion control is based on the Linear Matrix Inequalities (LMI) method, implemented using the Mathworks and Yalmip libraries. The results of controlling the ship's motion in accordance with the calculated trajectory are presented in the paper. With the use of the developed system, the ship can move autonomously based on the information from the DGPS system and a gyrocompass. The presented results concerned a computer simulation of maneuvers in the port of the Blue Lady ship from the Foundation for Shipping Safety and Environmental Protection.**

***Keywords*—autonomous ship; Ant Colony Optimization; Linear Matrix Inequalities; ship motion control; safe navigation**

I. Introduction

THE dynamic development of technology, observed in the recent years in the fields of automation and electronics, lead to the progress in the areas of unmanned and fully autonomous vehicles, such as Unmanned Aerial Vehicles (UAVs), self-driving cars, autonomous mobile robots, as well Autonomous Underwater Vehicles (AUVs). In the marine environment, smaller crafts operating on the surface of the water are called Unmanned Surface Vehicles (USVs), while larger vessels are named Maritime Autonomous Surface Ships (MASSs).

These vehicles might operate at different levels of autonomy. The International Maritime Organization (IMO), which is an agency of the United Nations responsible for defining regulations related to the shipping industry, formulate four degrees of autonomy. Degree one, is characterized by the lowest level of autonomy, where the seafarers on board operate and control the ship. Some processes and operations might be automated and some decision support systems may be used, but seafarers at all times are ready to take control. Degree two is a remotely controlled ship with seafarers on board. The ship is controlled remotely from a different location, such as the Shore Control Center, but the seafarers are ready to take control, if needed. In the degree three, the ship is controlled remotely and the seafarers are not present on board. The highest degree four is a fully autonomous ship, where the ship motion control system determines actions on its own, without any human intervention.

Over the years, methods allowing for the automatization of the different tasks performed during the ship operation, such as navigation and maneuvering, mooring and anchoring, have been developed. Recent approaches for solving the collision avoidance problem of autonomous ships include the application of the Velocity Obstacle (VO) algorithm combined with the Model Predictive Control (MPC) [1], the algorithm utilizing the isochrone method [2] and many approaches based on machine learning, such as the Deep Reinforcement Learning (DRL) [3], the Inverse Reinforcement Learning (IRL) [4], Multi-Agent Reinforcement Learning (MARL) [5] and fuzzy logic [6], [7]. Other recently proposed methods were based on swarm intelligence, such as the Beetle Antennae Search (BAS) algorithm [8] and the hybrid method based on the Artificial Potential Field (APF) and the Ant Colony Optimization (APF-ACO) algorithm [9].

The configuration of the MASS control system was formulated in [10], [11]. The system for cooperative navigation and control of USVs was introduced in [12]. The concept of formation control based on the Artificial Potential Field method and the results of field experiments in inland water environment were presented in the paper.

The aim of the research presented in this paper was to develop path planning and motion control methods for the implementation on board a ship in order to achieve the autonomous operation of the vessel. The following sections of the paper present the consecutive stages of tasks that have to be solved in order to develop an autonomous navigation system for the specified vessel. The next section presents the parameters of the vessel used in the research. Afterwards, a general diagram of the ship motion control system is shown and briefly described. Then, the following steps, leading to the development of a solution for autonomous operation of the vessel, are introduced and followed by an example of obtained results. The achievements of the presented research

This work was supported by the grants No. WE/2024/PZ/02 and WE/2024/PZ/03, financed from the internal science fund of the Faculty of Electrical Engineering, Gdynia Maritime University.

M. Rybczak and A. Lazarowska are with Department of Ship Automation, Faculty of Electrical Engineering, Gdynia Maritime University, Gdynia, Poland (e-mail: m.rybczak@we.umg.edu.pl, a.lazarowska@we.umg.edu.pl).

are summarized in the conclusions section along with the proposals of future research directions.

II. Parameters of the control object

In the research presented in this paper the control object is a ship model simulated in the Mathworks Matlab/Simulink 2022b environment. "Blue Lady" – the ship model presented in Fig. 1. – was made in relation to the actual ship in a scale of 1:24. The works [13]–[15] presented in detail the parameters of the training ship. The dimensions of the ship model are: the length: 13.75 m and the width: 2.38 m. The ship is steered with the use of two thrusters (bow and stern), two tunnel rudders (bow and stern), the main screw propeller and a fin rudder. The dynamics of the "Blue Lady" training ship were modelled in a digital form using the Simulink environment. The markings refer to the contents of matrices A, B, C and D of the nominal model.

Fig. 1. The training ship "Blue Lady" in the port on Lake Silm in Iława Kamionka

The "Blue Lady" training ship is a highly non-linear and multidimensional control object. The developed model of the control object included the ship's dynamics and kinematics, the Kalman filter system reproducing the vessel's speed and the thrust allocation. The three input signals to the control object include: τ_x – desired force (thrust) in the longitudinal axis of the ship; τ_y – desired force (thrust) in the transverse axis of the ship; τ_p – desired torque. The three output signals include: the $x(t)$ and $y(t)$ position coordinates and the heading of ship $\psi(t)$. The linearization of the multidimensional model of the control object was achieved experimentally. It consisted of the identification of the structure and values of the coefficients of the linear model. The state equations presented in the state space are as follows:

$$\begin{bmatrix} \dot{x_1} \\ \dot{x_2} \\ \dot{x_3} \end{bmatrix} = \begin{bmatrix} a_{uu} & 0 & 0 \\ 0 & a_{vv} & a_{vr} \\ a_{ru} & a_{rv} & a_{rr} \end{bmatrix} \cdot \begin{bmatrix} x_1 \\ x_2 \\ x_3 \end{bmatrix} + \begin{bmatrix} b_{uu} & 0 & 0 \\ 0 & b_{vv} & b_{vr} \\ b_{ru} & b_{rv} & b_{rr} \end{bmatrix} \cdot \begin{bmatrix} \tau_x \\ \tau_y \\ \tau_r \end{bmatrix} \quad (1)$$

$$\begin{bmatrix} u \\ v \\ r \end{bmatrix} = \begin{bmatrix} 1 & 0 & 0 \\ 0 & 1 & 0 \\ 0 & 0 & 1 \end{bmatrix} \cdot \begin{bmatrix} x_1 \\ x_2 \\ x_3 \end{bmatrix} \quad (2)$$

The matrices of the training ship considered as a control object have the following form:

$$A = \begin{bmatrix} -3.36 \cdot 10^{-5} & 0 & 0 \\ 0 & -9.0 \cdot 10^{-3} & -2.0 \cdot 10^{-4} \\ -3.0 \cdot 10^{-3} & -1.0 \cdot 10^{-2} & -7.75 \cdot 10^{-3}, \end{bmatrix} \quad (3)$$

$$B = \begin{bmatrix} -3.62 \cdot 10^{-3} & 0 & 0 \\ 0 & 2.06 \cdot 10^{-3} & -1.28 \cdot 10^{-5} \\ 3.00 \cdot 10^{-5} & 1.15 \cdot 10^{-5} & 8.00 \cdot 10^{-3}, \end{bmatrix} \quad (4)$$

$$C = \begin{bmatrix} 1 & 0 & 0 \\ 0 & 1 & 0 \\ 0 & 0 & 1 \end{bmatrix}, D = \begin{bmatrix} 0 & 0 & 0 \\ 0 & 0 & 0 \\ 0 & 0 & 0 \end{bmatrix}. \quad (5)$$

III. Ship motion control – case study

The paper presents the steps that need to be followed in order to perform computer simulations in the process of the algorithms' development for autonomous ship control.

A. Step 1 – Object identification

The computer simulation must reflect the ship's mathematical model. The process of collecting data related to the identification involves conducting a sufficient number of experiments using a simulation model with various configurations of input and output signals to the object: MIMO, MISO or SISO. In this process the Matlab package and its "System Identification Toolbox" library were used. The model coefficients were calculated based on the Prediction Error Method (PEM). The sources of input signal were defined using the "Band Limited White Noise" blocks, setting the period of the amplitude signal changes and the value in the "pseudo-random number generator kernel" mode. The value of the amplification factor was selected in a given path in order to obtain similar values of the standard deviation of individual signals for different values of the amplitude change period. The waveforms of the input and output signals obtained in this way were stored in each trial. The quality of the model coefficients was verified using the autocorrelation functions of the model output signals and the cross-correlation functions of the input and output signals. To determine the degree of matching of the model's output signals to the verification signal, the relationship from the L. Ljung source *System Identifiction Toolbox ver.5.* was used:

$$F_{it\%} = \left[1 - \frac{\sigma^2(q_m - \hat{q}_m)}{\sigma^2(q_m - \bar{q}_m)}\right] \cdot 100\% \quad (6)$$

where: q_m - verification signal, $\bar{q}_m$ - mean value, $\hat{q}_m$ - output of the model.

During the experiments, deviations of 20% from the coefficient value were rejected. As a result of the performed tests, the coefficient values were obtained for matrices A and B of the model of the object. Maximum and minimum values were obtained for each coefficient and were presented in the

works [16], [17]. Moreover, it was noticed that the dynamics of the individual tracks of the obtained nominal model is satisfactory for non-zero coefficients.

B. Step 2 – Safe trajectory planning with the use of the Ant Colony Optimization

In the research presented in this paper the collision avoidance and path planning problem of autonomous ships was solved with the use of one of the most popular swarm intelligence method – the Ant Colony Optimization (ACO). The ship's safe path planning can be divided into global and local navigation, also known as deliberative and reflexive (or reactive) path planning. The division of approaches comes from robotics and depends on the type of information about the environment considered in the calculations, particularly the type of obstacles. Deliberative approaches are aimed at planning a path from a starting position to a goal location based on the map of the environment. In reactive path planning the path is being planned and re-planned based on the data continuously received from sensors. The path is updated based on current data about the environment, when it is needed, e.g. when a new dynamic obstacle has been detected in the close surroundings.

In the autonomous shipping, the information about the environment is obtained from different navigational aids, such as the Automatic Identification System (AIS), radars with the Automatic Radar Plotting Aid (ARPA), the GPS, echosounders, logs and gyrocompasses. These data can be integrated and displayed using the Electronic Chart Display and Information System (ECDIS). The static obstacles in the marine environment are lands, shallows, fishing nets, buoys or military zones. The dynamic obstacles are the target ships, which are vessels, that might pose a risk of collision and therefore needs to be avoided. A safe path also has to be compliant with the International Regulations for Preventing Collisions at Sea (COLREGs).

In the process of ship's path planning an optimization algorithm determines a safe path P from the current position of an own ship to the defined final position (waypoint). The safe path should be characterized by the smallest possible deviation from the current track. The safe path P, composed of $(e+1)$ waypoints from the initial waypoint wp_0 (current position of an own ship) to the final waypoint wp_f, can be defined by Equation 7). Every waypoint is defined by the coordinates of the ship's position (x and y) and the ship's course ψ (and possibly speed V).

$$P = \{wp_0 = [x_0, y_0, \psi_0], wp_1 = [...], ..., wp_f = [x_f, y_f, \psi_f],\} \tag{7}$$

The path planning algorithm applied in the described research calculated a safe path between the current position of an own ship and the defined final position, considering the static navigational restrictions. Static obstacles were modeled as polygons. Based on the data concerning the location of static obstacles and the position of an own ship, a graph composed of possible own ship's turning points is constructed in the solution space. In this process, the vertices of the graph that are inside the areas occupied by the obstacles, are removed from the graph. Afterwards, the calculation of an own ship's safe path, using ACO-based algorithm, is carried out. It consists of three main stages: the ACO data initialization, the solutions construction by artificial ants and the pheromone trail update procedure.

In the ACO data initialization these parameters of the ACO algorithm are initialized:

- an initial value of the pheromone trail tau_0 on all of the vertices,
- the α and β coefficients, used in the formula for the probability of the ant's next move,
- the pheromone evaporation rate ρ (0 ¡ ρ ¡= 1),
- the number of artificial ants,
- the maximum number of the ant's steps, and
- the number of iterations.

$$P^{ant}_{wp_{ij}}(t) = \frac{[\tau_{wp_j}(t)]^{\alpha} \cdot [\eta_{wp_{ij}}]^{\beta}}{\sum_{l \in wp^{ant}_i} [\tau_{wp_l}(t)]^{\alpha} \cdot [\eta_{wp_{il}}]^{\beta}} \tag{8}$$

The solutions construction by artificial ants is composed of the following steps:

1) Every artificial ant starts the construction of its path from the initial vertex wp_0 with coordinates (x_0, y_0), which is the current position of an own ship;
2) Afterwards every ant constructs its path until it has reached the final vertex wp_f with the coordinates (x_f, y_f) or it has reached the maximum number of steps; in every step the ant selects the next vertex from the neighboring vertices in a probabilistic manner, using the action choices rule. The selection of the next vertex depends on the value of the pheromone trail on vertex j adjacent to the current vertex i - $\tau_j(t)$ and a heuristic information η_{ij}, which is calculated as an inverse of the distance between the current vertex i and the neighboring vertex j. The probabilistic selection of the next vertex works similarly to the roulette wheel selection procedure applied in the evolutionary algorithms. Equation 8 is applied for the calculation of the selection probability of the next vertex from the neighboring vertices. If the α coefficient, used in this equation, is equal to 0, the most probable is the selection of the nearest next vertex, if the β coefficient is equal to 0, only the reinforcement of the pheromone trail amount is applied.

$$\tau_{wp_j}(t+1) = (1-\rho) \cdot \tau_{wp_j}(t) + \sum_{ant=1}^{ant\_num} \Delta\tau^{ant}_{wp_j}(t) \tag{9}$$

After all of the ants in the iteration have finished constructing their paths, the pheromone trail update procedure, defined by Equation 9, is applied, it is composed of the following steps:

1) The pheromone evaporation, which is applied in order to reduce the pheromone trail on all vertices on the graph by some constant value;
2) The pheromone deposit, during which a certain value of the pheromone trail is added to all of the vertices on the

graph belonging to the paths constructed by the ants in the current iteration; it is applied in order to reinforce the selection probability of the vertices that are the parts of the paths chosen by many ants and that are the parts of the shortest paths. Before the next iteration, the best solution found so far is saved. The best solution is the shortest path. The termination condition of the algorithm is the maximum number of iterations.

C. Step 3 – the master controller

The master controller for the ship's trajectory to control the ship's movement in the low speeds range, transforms the trajectory and the given course into the signals of longitudinal, lateral and angular speeds. A detailed description of the system's operation is provided in the works [16], [18]. The principle is based on the mathematical calculations that are represented by a set of numbers: the coordinate values of the next waypoint of the trajectory and the ship's course on the section to this point: $[x_1,y_1,\ \psi_1]$, $[x_n,y_n,\psi_n]$, $[x_{n+1},y_{n+1},\psi_{n+1}]$. For every point and the difference between the current point and the next one, the speed is calculated. Fig. 2 presents three main areas in which the trajectory controller works. The position of the ship in relations to the next waypoint of the trajectory is determined. The current trajectory of the ship besides the current section of the trajectory (dashed line) is determined by the angle ρ, which in turn determines the maximum values u_{max} and v_{max}. There are 3 areas of the ellipse marked in this figure. If the ship is in a given area, it starts to enforce the speed control. Special attention should be paid to the location of area I, which enforces the maximum value for the assigned speed to be reached, after being in area II, it drops slightly from the value on the longitudinal and lateral speed signal, and when the ship is in the area for ellipse III, it "goes down" to the minimum value, i.e. the ship reaches its point and can move to the next waypoint on the trajectory section. It is important that for all areas: I, II and III the behavior towards longitudinal and lateral speed is symmetrical, i.e. depending on the point at which the ship is located, the controller calculates the possibility of changing the speed signal.

For a training ship, whose dimensions are about 14 meters of length and about 2.5 meters of width, it is difficult to enter area III. The speed signals generated in this way are the set ones for the slave LMI controller.

D. Step 4 – LMI controller

The slave controller is the ship's low speed controller, aimed at determining the forces needed to control the ship's propulsors. The controller is based on the solutions of Linear Matrix Inequalities. The presented state controller with gain was developed on the basis of the principle of the poles' placement in the left half-plane and based on the energy leveling of the set signal. It is possible to control the ship based on measurements of the ship's position, the calculations should consider the disturbances of the process, the measurements of wind and waves.

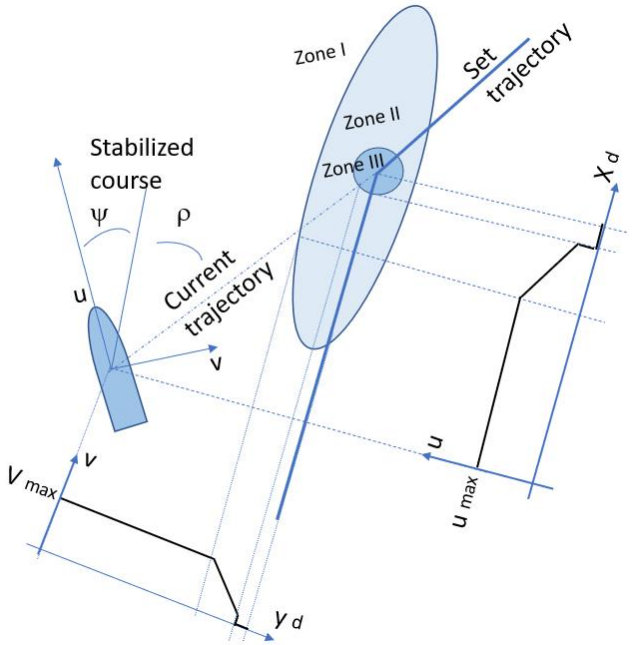

Fig. 2. The principle of operation of the master controller [18]

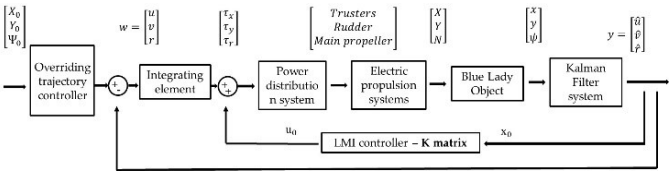

Fig. 3. A block diagram of the control system for an autonomous ship

Multidimensional control applies to many issues related to the ship automation, but in this example it concerns the control for three variables that cannot influence other control variables in the form of so-called cross-coupling. In the presented example, the object is non-linear, while the matrices are linear. In this case, linearity around the operating point is determined. In this part, the control of a multidimensional object is designed based on the linear matrix inequalities. For the dependence of the derivative of the state variable on the main matrix **A** of the autonomous linear system, the following was entered:

$$\dot{x} = Ax \tag{10}$$

A necessary and sufficient condition for a linear system to be stable is the existence of a symmetric and positive definite **X** matrix for the inequality:

$$A^T X + AX \prec 0 \tag{11}$$

where A – the matrix of the linear system, X – the searched matrix, symmetrical, positive definite.

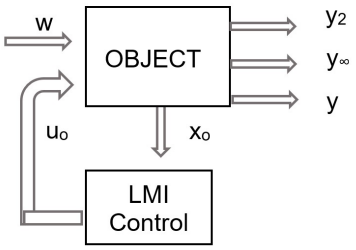

Fig. 4. The concept of the LMI controller

Based on simulation results controller structure (Fig. 3 and Fig. 4) based on a state space controller was chosen, as:

$$u_o = K \cdot x_o \tag{12}$$

Closed loop system state space equations have the form of:

$$\begin{cases} \dot{x_o} = (A + B_u K)x_o + B_w w, x_o = \begin{bmatrix} x_i \\ x \end{bmatrix} \\ y = (C + D_{yu}K)x_o + D_{yw}w \\ y_\infty = (C_\infty + D_{\infty u}K)x_o + D_{\infty y}w \\ y_2 = (C_2 + D_{2u}K)x_o + D_{2w}w \end{cases} \tag{13}$$

- A – controlled object state space matrix; - B_u – control matrix control matrix of control $'u'$ signal; - B_{ww} – control matrix of input $'w'$ signal; - C – output matrix of output signal $'y'$; - C_∞ - output matrix of $'y'_\infty$ signal;+ - C_2 - output matrix of $'y'_2$ signal; - D_{zu} - transition matrix of $'y'$ and $'u'$ signals; - D_{zw} - transition matrix of $'y'$ and $'w'$ signals; - $D_{\infty u}$ - transition matrix of $'y'_\infty$ and $'u'$ signals; - $D_{\infty w}$ - transition matrix of $'w'$ and $'y'_\infty$ signals; - D_{2u} - transition matrix of $'y'_2$ and $'u'$ signals; - D_{2w} - transition matrix of $'y'_2$ and $'w'$ signals.

Additionally, referring to Schur's Lemma (2.8 in [19]), it can be noted that:

$$M = \begin{bmatrix} A & B \\ B^T & D \end{bmatrix} \tag{14}$$

The algebraic Riccati inequality in non-linear (Theorem 5.4 in [19]) form taking into account Schur's complement can be written as:

$$\begin{bmatrix} A^T X + XA + Q & XB \\ B^T & R \end{bmatrix} \prec 0 \tag{15}$$

In an object prepared in such way, three stages of the process of the controller design are performed. The first is related to defining the area of poles distribution in the left half-plane of the complex variable s in order to determine the dynamic parameters of the designed closed-loop system [20]. The relevant calculations are presented, in the work [21] however, the area of pole placement between the two belts (α_1 and α_2) is written in the form:

$$D_{\alpha_1,\alpha_2} = \{s; \alpha_1 < Re(s) < \alpha_2\} \tag{16}$$

If for:

$$Re(s) = \frac{1}{2}(s + \bar{s}), \tag{17}$$

then the area is defined as:

$$D_{\alpha_1,\alpha_2} = \left\{s; \alpha_1 < \frac{1}{2}(s + \bar{s}) < \alpha_2\right\}, \tag{18}$$

so:

$$D_{\alpha_1,\alpha_2} = \left\{s; \frac{1}{2}\begin{bmatrix} s & 0 \\ 0 & -s \end{bmatrix} + \frac{1}{2}\begin{bmatrix} \bar{s} & 0 \\ 0 & -\bar{s} \end{bmatrix} + \begin{bmatrix} \alpha_1 & 0 \\ 0 & -\alpha_2 \end{bmatrix} < 0\right\} \tag{19}$$

If:

$$L = \begin{bmatrix} \alpha_1 & 0 \\ 0 & -\alpha_2 \end{bmatrix}, M = \begin{bmatrix} 1 & 0 \\ 0 & -1 \end{bmatrix}, \tag{20}$$

$$\begin{aligned} R_{zone}(A, X_{zone}) = L \otimes X_{zone} + M \otimes (AX_{zone}) \\ + M^T \otimes (AX_{zone})^T \prec 0 \end{aligned} \tag{21}$$

Based on the above considerations, the gain controller at this stage satisfies the relationship:

$$K_{zone} = Y_{zone} \cdot X_{zone}^{-1} \tag{22}$$

The second stage is the minimization of the control error, i.e. the minimization of the H_∞ norm (Theorem 5.4 in [19]):

$$\begin{bmatrix} X_\infty A^T + AX_\infty & B & XC^T \\ B^T & -\gamma_\infty I & D^T \\ CX & D & -\gamma_\infty I \end{bmatrix} \prec 0 \tag{23}$$

The state controller synthesis problem has a solution if the second step of LMI is satisfied. Invoking the property about the existence of the inverse of a matrix:

$$K_\infty = Y_\infty \cdot X_\infty^{-1} \tag{24}$$

The third stage is the H2 minimization, i.e. designing a controller, whose main goal is to minimize the energy of the control signal ([lemma 2.13 in [19]):

$$\begin{cases} \begin{bmatrix} AX_2 + X_2 A^T & B \\ B^T & -I \end{bmatrix} \prec 0 \\ \begin{bmatrix} Q & C^T \\ C & X_2 \end{bmatrix} \succ 0 \\ Tr(Q) < \gamma_2^2 \end{cases} \tag{25}$$

The synthesis of the controller focuses on finding the value of the gain matrix K for the state space controller:

$$K_2 = Y_2 \cdot X_2^{-1} \tag{26}$$

A number of calculations that need to be performed appeared in the works [Theorem 5.4 in [19]]. The paper uses conditions from Equations 16-26 and makes use of the Yalmip [22] and SeDuMi [23] library. The state matrix K for the state controller was determined based on the above dependencies and has the form:

$$K = 10^3 \cdot \begin{bmatrix} 1732 & 0.010 & 0.000 & -658 & 0.000 & -0.200 \\ -0.01 & 1564 & -3.80 & 0.00 & -897 & 6.0 \\ -5.40 & -2.801 & 421 & 3.40 & 1.400 & -234 \end{bmatrix} \tag{27}$$

IV. Results of Automatic Ship Steering Along a Determined Trajectory

After the completion of the above described five steps and entering data into the mathematical model of the ship control system in the Simulink environment, simulations were carried out for an exemplary ship's safe trajectory calculated using the ACO algorithm. It was confirmed that using the master trajectory controller and the state controller based on the Linear Matrix Inequalities, it is possible to autonomously control the training vessel in limited waters in the port of Lake Silm in Iława. An example of a safe path determined by the ACO-based algorithm with the use of the parameters' values listed in Table I is shown in Fig. 5.

TABLE I
ACO Parameters Used in the Simulation Tests

Parameter	Value
α	0.5
β	0.5
ρ	0.5
τ_0	0.001
number of ants	300
number of iterations	20

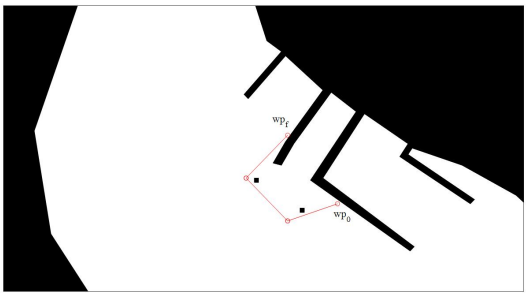

Fig. 5. An example of a safe path calculated with the use of the ACO-based algorithm

Reading the ship's input parameters such as position, i.e. DGPS, and position according to the gyro compass information allows the ship to be steered, so the presented safe trajectory in port was entered into the system and the "Blue Lady" ship executed the maneuver presented in Fig. 6.

The maneuver involves bouncing off the quay, then changing course from 121 to 325 allows the vessel to turn and enter the second quay. The whole process in the simulation takes about 3,000 seconds, or as much as an hour, the corresponding diagram for the three longitudinal, transverse and angular speeds is presented in Fig. 7.

During the maneuver, the values for the ship's propulsion system, i.e. the tunnel thruster and the bow and stern thrusters respectively, were read out, as shown in Fig. 8.

V. Conclusions

When doing research, scientists often focus on a slice of work, this article presents a case study for determining the

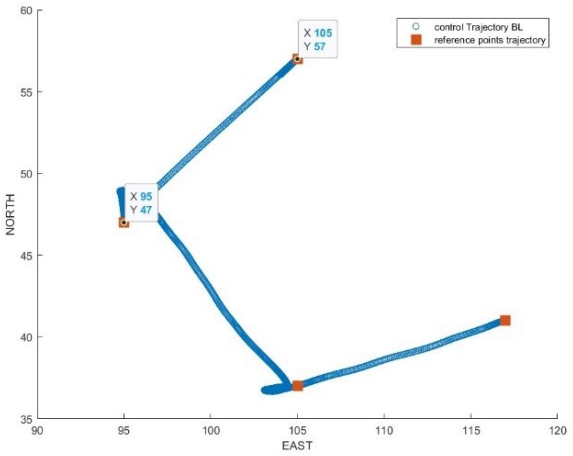

Fig. 6. The executed trajectory of the ship for the test example, the red point is number x, y and ψ, blue line is the trajectory of the ship

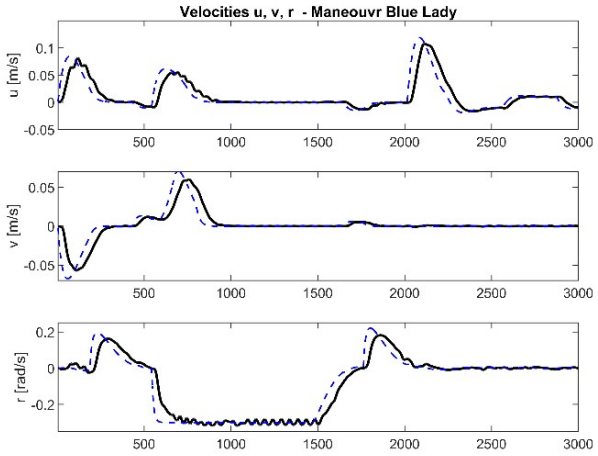

Fig. 7. The velocities u, v, r of the ship during the ship's movement along the calculated trajectory

safe trajectory of a vessel in a port. All of the vital steps, needed to be performed in order to develop a system for automatic ship control in a port, were described in the paper along with an example of obtained results. These tasks include: the ship's mathematical model identification, the development of a safe trajectory planning algorithm, the development of the master controller transforming the trajectory into the signals of longitudinal, lateral and angular speeds and the development of the ship's low speed controller. The paper also introduced the sensors needed in order to provide all of the input data to the system, such as e.g. the DGPS and the gyrocompass.

According to the authors, the results apply to the automatic control of a vessel. The simulations proved that operations based on electronic measurements and by controlling the ship's propulsion systems allow full compatibility to obtain the above results. An important point in the future research will be the verification of this maneuver under real conditions

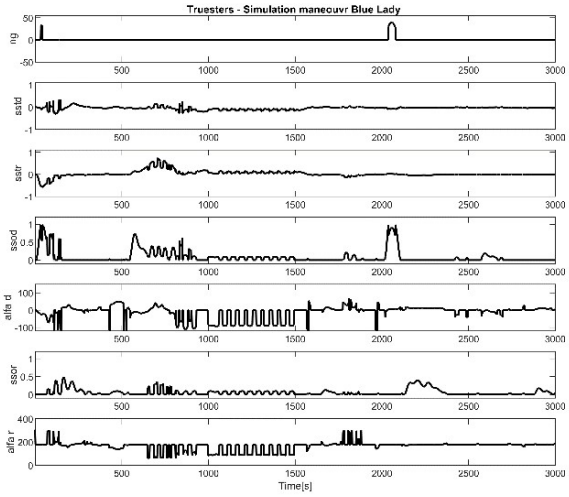

Fig. 8. List of thruster signals: ng, main propeller; sstd, relative thrust of the bow tunnel thruster; sstr, relative thrust of the stern tunnel thruster; ssod, relative thrust of the bow rotary thruster; alfa d (α_d), bow rotary thruster deflection angle; ssor, relative thrust of the stern rotary thruster; alfa r (α_r), stern rotary thruster deflection angle

in the port of Iława on Lake Silm at the Foundation for Navigation Safety and Environmental Protection. Future research directions might also include the application of machine learning methods in the process of the automatic control system development.

REFERENCES

[1] K. Zhang, L. Huang, Y. He, B. Wang, J. Chen, Y. Tian, and X. Zhao, "A real-time multi-ship collision avoidance decision-making system for autonomous ships considering ship motion uncertainty," *Ocean Engineering*, vol. 278, p. 114205, 2023. [Online]. Available: https://www.sciencedirect.com/science/article/pii/S0029801823005899

[2] D. Kim, J.-S. Kim, J.-H. Kim, and N.-K. Im, "Development of ship collision avoidance system and sea trial test for autonomous ship," *Ocean Engineering*, vol. 266, p. 113120, 2022. [Online]. Available: https://www.sciencedirect.com/science/article/pii/S0029801822024039

[3] D.-H. Chun, M.-I. Roh, H.-W. Lee, and D. Yu, "Method for collision avoidance based on deep reinforcement learning with path-speed control for an autonomous ship," *International Journal of Naval Architecture and Ocean Engineering*, vol. 16, p. 100579, 2024. [Online]. Available: https://www.sciencedirect.com/science/article/pii/S2092678223000687

[4] M. Zheng, S. Xie, X. Chu, T. Zhu, and G. Tian, "Research on autonomous collision avoidance of merchant ship based on inverse reinforcement learning," *International Journal of Advanced Robotic Systems*, vol. 17, no. 6, p. 1729881420969081, 2020. [Online]. Available: https://doi.org/10.1177/1729881420969081

[5] G. Wei and W. Kuo, "Colregs-compliant multi-ship collision avoidance based on multi-agent reinforcement learning technique," *Journal of Marine Science and Engineering*, vol. 10, no. 10, 2022. [Online]. Available: https://www.mdpi.com/2077-1312/10/10/1431

[6] J. Lisowski and M. Mohamed-Seghir, "Comparison of computational intelligence methods based on fuzzy sets and game theory in the synthesis of safe ship control based on information from a radar arpa system," *Remote Sensing*, vol. 11, no. 1, 2019. [Online]. Available: https://www.mdpi.com/2072-4292/11/1/82

[7] M. Mohamed-Seghir, "The fuzzy properties of the ship control in collision situations," in *2017 IEEE International Conference on INnovations in Intelligent SysTems and Applications (INISTA)*, 2017, pp. 107–112.

[8] S. Xie, X. Chu, M. Zheng, and C. Liu, "Ship predictive collision avoidance method based on an improved beetle antennae search algorithm," *Ocean Engineering*, vol. 192, p. 106542, 2019. [Online]. Available: https://www.sciencedirect.com/science/article/pii/S0029801819306766

[9] M. Li, B. Li, Z. Qi, J. Li, and J. Wu, "Optimized apf-aco algorithm for ship collision avoidance and path planning," *Journal of Marine Science and Engineering*, vol. 11, no. 6, 2023. [Online]. Available: https://www.mdpi.com/2077-1312/11/6/1177

[10] T. Zubowicz, K. Armiński, A. Witkowska, and R. Śmierzchalski, "Marine autonomous surface ship - control system configuration," *IFAC-PapersOnLine*, vol. 52, no. 8, pp. 409–415, 2019, 10th IFAC Symposium on Intelligent Autonomous Vehicles IAV 2019. [Online]. Available: https://www.sciencedirect.com/science/article/pii/S2405896319304343

[11] W. Koznowski, K. Kula, A. Lazarowska, J. Lisowski, A. Miller, A. Rak, M. Rybczak, M. Mohamed-Seghir, and M. Tomera, "Research on synthesis of multi-layer intelligent system for optimal and safe control of marine autonomous object," *Electronics*, vol. 12, no. 15, 2023. [Online]. Available: https://www.mdpi.com/2079-9292/12/15/3299

[12] J. Park, M. Kang, Y. Lee, J. Jung, H.-T. Choi, and J. Choi, "Multiple autonomous surface vehicles for autonomous cooperative navigation tasks in a marine environment: Development and preliminary field tests," *IEEE Access*, vol. 11, pp. 36 203–36 217, 2023.

[13] M. Tomera, "Dynamic positioning system design for "blue lady". simulation tests," *Polish Maritime Research*, vol. 19, no. Special, pp. 57–65, 2012.

[14] ——, "Hybrid real-time way-point controller for ships," in *2016 21st International Conference on Methods and Models in Automation and Robotics (MMAR)*, 2016, pp. 630–635.

[15] J. Pomirski, A. Rak, and W. Gierusz, "Control system for trials on material ship model," *Polish Maritime Research*, vol. 19, no. Special, pp. 25–30, 2012. [Online]. Available: https://doi.org/10.2478/v10012-012-0019-1

[16] W. Gierusz, N. Cong Vinh, and A. Rak, "Maneuvering control and trajectory tracking of very large crude carrier," *Ocean Engineering*, vol. 34, no. 7, pp. 932–945, 2007. [Online]. Available: https://www.sciencedirect.com/science/article/pii/S0029801806001831

[17] W. Gierusz, "Simulation model of the shiphandling training boat "blue lady"," *IFAC Proceedings Volumes*, vol. 34, no. 7, pp. 255–260, 2001, iFAC Conference on Control Applications in Marine Systems 2001, Glasgow, Scotland, 18-20 July 2001. [Online]. Available: https://www.sciencedirect.com/science/article/pii/S1474667017350929

[18] M. Rybczak and W. Gierusz, "Maritime autonomous surface ships in use with lmi and overriding trajectory controller," *Applied Sciences*, vol. 12, no. 19, 2022. [Online]. Available: https://www.mdpi.com/2076-3417/12/19/9927

[19] H.-H. Y. Guang-Ren Duan, *LMIs in Control Systems: Analysis, Design and Applications*. Boca Raton, FL, USA: CRC Press, 2013.

[20] S. Boyd, L. El Ghaoui, E. Feron, and V. Balakrishnan, *Linear Matrix Inequalities in System and Control Theory*. SIAM studies in applied mathematics: 15, 1994.

[21] M. Rybczak, "Improvement of control precision for ship movement using a multidimensional controller," *Automatika*, vol. 59, pp. 63 – 70, 2018. [Online]. Available: https://api.semanticscholar.org/CorpusID:116052877

[22] Yalmpi library. [Online]. Available: https://yalmip.github.io/download

[23] J. F. Sturm, "Using sedumi 1.02, a matlab toolbox for optimization over symmetric cones," *Optimization Methods and Software*, vol. 11, no. 1-4, pp. 625–653, 1999. [Online]. Available: https://doi.org/10.1080/10556789908805766